

Parsec-scale structure in the warm ISM from polarized galactic radio background observations

M. Haverkorn*, P. Katgert* and A. G. de Bruyn†

*Leiden Observatory, P.O. Box 9513, 2300 RA Leiden, the Netherlands

†ASTRON, P.O. Box 2, 7990 AA Dwingeloo, the Netherlands

Abstract. We present multi-frequency polarization observations of the diffuse radio synchrotron background modulated by Faraday rotation, in two directions of positive latitude. No extended total intensity I is observed, which implies that total intensity has no structure on scales smaller than approximately a degree. Polarized intensity and polarization angle, however, show abundant small-scale structure on scales from arcminutes to degrees. Rotation Measure (RM) maps show coherent structure over many synthesized beams, but also abrupt large changes over one beam. RM's from polarized extragalactic point sources are correlated over the field in each of the two fields, indicating a galactic component to the RM, but show no correlation with the RM map of the diffuse radiation. The upper limit in structure in I puts constraints on the random and regular components of the magnetic field in the galactic interstellar medium and halo. The emission is partly depolarized so that the observed polarization mostly originates from a nearby part of the medium. This explains the lack of correlation between RM from diffuse emission and from extragalactic point sources as the latter is built up over the entire path length through the medium.

INTRODUCTION

Synchrotron radiation emitted in our galaxy provides a diffuse radio background, which is altered by Faraday rotation and depolarization when it propagates through the galactic halo and interstellar medium. Multi-frequency observations of the linearly polarized component of this radio background allow determination of the Rotation Measure (RM) of the medium along many contiguous lines of sight, from which the structure of the small-scale galactic magnetic field, weighted with electron density, can be probed. After the discovery paper ([1]), many other high resolution radio background observations have shown intriguing polarization structure, mostly in the galactic plane ([2], [3], [4], [5]). Here, we focus on regions of positive galactic latitude to evade complexities such as HII regions, supernova remnants etc. Furthermore, these are sensitive and multi-frequency observations so that accurate RM values can be determined.

OBSERVATIONS

With the Westerbork Synthesis Radio Telescope (WSRT) we mapped the polarized radio background in two fields of over 50 square degrees each in the second galactic quadrant at positive latitudes. All four Stokes parameters I , Q , U , and V were imaged in five frequency bands centered at 341, 349, 355, 360, and 375 MHz simultaneously (bandwidth 5 MHz), at a resolution of $\sim 4'$. The first field, in the constellation Auriga, is $7^\circ \times 9^\circ$ in size and centered on $(l, b) = (161, 16)^\circ$; the second field, in the constellation Horologium, is $8^\circ \times 8^\circ$ wide and centered on $(l, b) = (137, 7)^\circ$. No total intensity I was detected (besides point sources) in either field down to ~ 0.7 K, which is $< 1.5\%$ of the expected sky brightness in these regions, indicating that I does not vary on scales detectable to the interferometer, i.e. below about a degree. However, linearly polarized intensity P and polarization angle φ show abundant small-scale structure. Other fields observed with the WSRT at a single frequency around 350 MHz also show small-scale structure in polarized intensity and polarization angle, but of very different topologies ([6]).

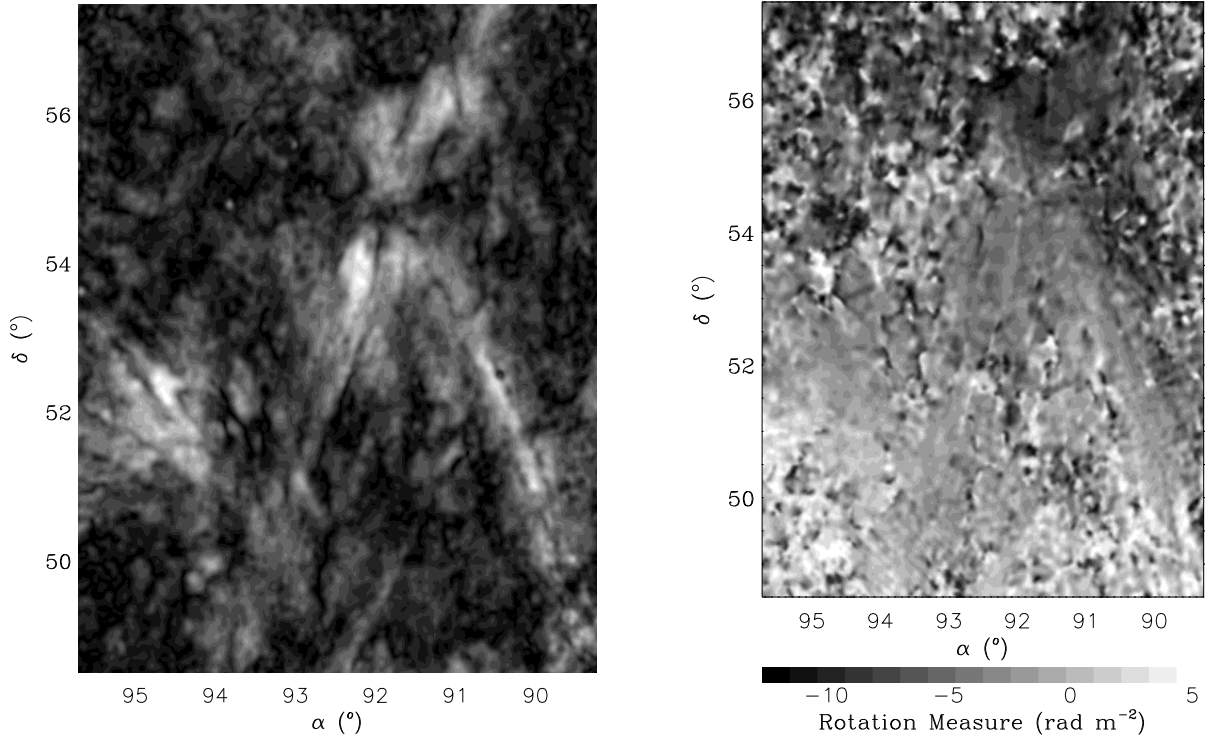


FIGURE 1. *Left:* polarized intensity P at 349 MHz in the Auriga field at $4'$ resolution. White denotes a maximum $T_{b,pol} \approx 18$ K. *Right:* RM in the Auriga field. Very high or low RM values ($|RM| \approx 30 - 60$ rad m^{-2}) in the field have been removed from the maps (see text).

ANALYSIS OF THE AURIGA FIELD

The structure in polarized intensity P in the Auriga field shows a wide variety in topology on several scales, as shown in the left plot of Fig. 1, where P at 349 MHz is mapped at $4'$ resolution. The typical polarization brightness temperature is $T_{b,pol} \approx 6 - 8$ K, with a maximum of ~ 18 K. From the Haslam continuum survey at 408 MHz ([7]), the I -background at 408 MHz in this region of the sky is ~ 33 K. Extrapolating this to our frequencies with a temperature spectral index of -2.5 between 341 MHz and 408 MHz ([8]), the total intensity background is $\sim 41 - 52$ K. So the maximum degree of polarization $p_{max} \approx 35\%$, with an average p of 15%.

In addition, a pattern of black narrow wiggly canals is visible (see e.g. the canal around $(\alpha, \delta) = (92.7, 49 - 51)^\circ$). These canals are all one synthesized beam wide and have been shown to separate regions of fairly constant polarization angle ϕ where the difference in ϕ is approximately 90° ($\pm n 180^\circ$, $n = 1, 2, 3 \dots$), which causes beam depolarization ([9]). The angle changes are due to abrupt changes in RM. Hence, the canals reflect specific features in the angle distribution. Other angle (and RM) changes within the beam cause less or no depolarization, so that they do not leave easily visible traces in the polarized intensity distribution.

The RM of the Faraday-rotating material can be derived from $\phi(\lambda^2) \propto RM \lambda^2$ (see [10] for details and pitfalls). The right plot in Fig. 1 gives a $4'$ resolution RM map of the Auriga field. The average RM ≈ -3.4 rad m^{-2} , and in general $|RM| < 15$ rad m^{-2} . Very high or low RM values ($|RM| \approx 30 - 60$ rad m^{-2}) in the field occur only at positions where polarized intensity P is very low, so noise errors in polarization angle are very large. Therefore the RM's at these positions are not reliable and have been removed from the maps. RM's show structure on scales of many beams (up to degree scales), but also abrupt changes from one beam to another. This is illustrated in the left map of Fig. 2, where a small part of the Auriga field is shown. Here, the lines are graphs of polarization angle against wavelength squared, so that the slope of the line is RM. Each graph is an independent synthesized beam. The greyscale denotes polarized intensity P at 349 MHz, five times oversampled. Large sudden RM changes occur: e.g. at $(\alpha, \delta) = (94.68, 53.15)^\circ$, RM changes from -9 rad m^{-2} to 7 rad m^{-2} , and at $(\alpha, \delta) = (94.60, 53.00)^\circ$ from 3 rad m^{-2} to -11 rad m^{-2} . A change in sign of RM indicates in general a change in *direction* of the galactic magnetic field along the line of sight, although

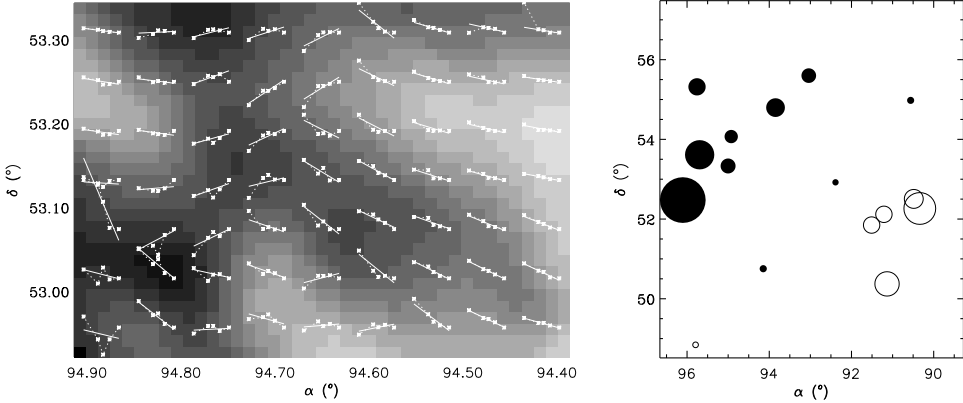


FIGURE 2. *Left:* Graphs of polarization angle against the square of the wavelength, so that the slope is RM. Each graph denotes an independent beam. The greyscale denotes polarized intensity at 349 MHz, five times oversampled. RM's range from ~ -10 to 10 rad m^{-2} , ignoring the one anomalously large negative RM on the left side. Abrupt changes in Rotation Measure over one beam ($4'$) are coherent along several beams. *Right:* RM's of observed polarized extragalactic point sources in the Auriga field. The radii of the circles are scaled with magnitude of RM, where filled circles are positive RM's. Maximum (minimum) RM is 19.5 (-13.6) rad m^{-2} .

numerical models of propagation of polarized radiation through a mixed (synchrotron emitting and Faraday-rotating) medium show a change of sign of RM also without a reversal in the magnetic field ([11]).

We detected seventeen polarized extragalactic sources in the Auriga field at a higher resolution ($\sim 1'$), with RM's from -13.6 to 19.5 rad m^{-2} . The right plot in Fig. 2 shows the RM's and positions of the sources, where the sizes of the circles are proportional to RM, and open (filled) circles denote negative (positive) RM's. The RM's of the extragalactic sources exhibit a clear gradient across the field of $\sim 5 \text{ rad m}^{-2}$ per degree roughly in the direction of galactic latitude, indicating a galactic component to the RM's of the sources. The change of sign over the field means a (local) reversal in the magnetic field parallel to the line of sight. We estimate a RM component intrinsic to the source of $< 5 \text{ rad m}^{-2}$, consistent with earlier estimates ([12]). The RM structure of the diffuse galactic radiation is independent from the observed RM of the extragalactic sources (see below).

ANALYSIS OF THE HOROLOGIUM FIELD

The left map in Fig. 3 shows polarized intensity at 349 MHz in the Horologium field. The average polarization brightness temperature is $\sim 5 \text{ K}$, and $T_{b, pol}$ in the ring-like structure is $\sim 11\text{-}15 \text{ K}$. The average degree of polarization is 5% and the maximum 25%, again derived using the Haslam survey ([7]). The ring with diameter $\sim 2.7^\circ$ is visible in all frequency bands, although the ring becomes more diffuse and smeared out towards higher frequencies and the left side is clearer than the right side. Beam-wide depolarized canals are again caused by beam depolarization. In the lower right, the depolarized canals are aligned along constant latitude. Caution is required in interpreting the P map, as the Horologium field is imbedded in a region of very high constant polarization ([13]). Due to missing small spacings, we cannot detect this large-scale component in Q and/or U , which causes a distorted image in P as well as RM. Possible solutions to this problem will be given in a forthcoming paper. A ring in P was also detected by Verschuur ([14]) at $40'$ resolution with a single dish, although not as an enhancement but as a deficiency in P .

In the RM map of the Horologium field (the right hand map of Fig. 3), a circular structure is clearly visible, which is slightly bigger than the ring in polarized intensity. Inside this RM disk, RM's decrease from the edge of the ring to the center, from ~ 0 to -10 rad m^{-2} . Outside the disk, RM's vary around zero without a clear gradient, with a maximum of $\sim 7 \text{ rad m}^{-2}$. Note that if P is low outside the disk, the influence of undetected large-scale polarization becomes larger and RM's may not be well-determined. The left and center plots of Fig. 4 give horizontal cross sections through the center of the RM disk and through the P ring at 349 MHz at the same position. The decrease in RM within the RM disk can be modeled with a homogeneous sphere of constant electron density and magnetic field. For values of electron density $n_e = 0.03 \text{ cm}^{-3}$ and parallel magnetic field $B_{\parallel} = 2 \mu\text{G}$, the distance to the sphere is about 300 pc.

In the Horologium field, we detected 18 polarized extragalactic point sources as shown in the right plot of Fig. 4.

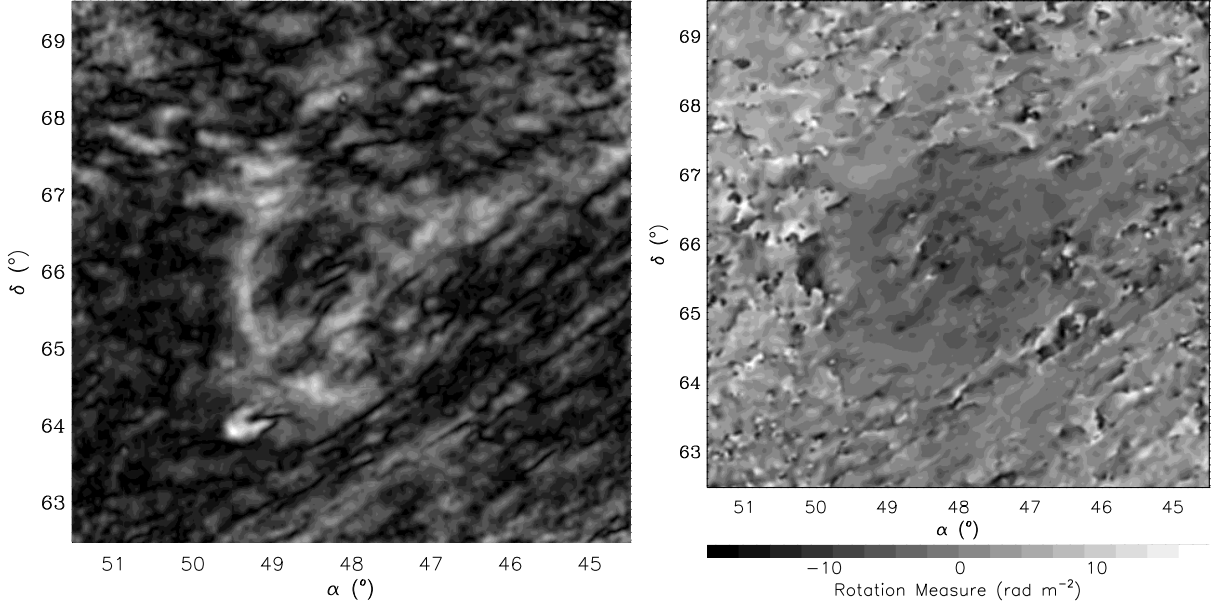


FIGURE 3. *Left:* polarized intensity P at 349 MHz in the Horologium field at $4'$ resolution. White denotes a maximum $T_{b, pol} \approx 15$ K. *Right:* RM in the Horologium field. Very high or low RM values ($|RM| \approx 30 - 60$ rad m $^{-2}$) in the field have been removed from the maps (see text).

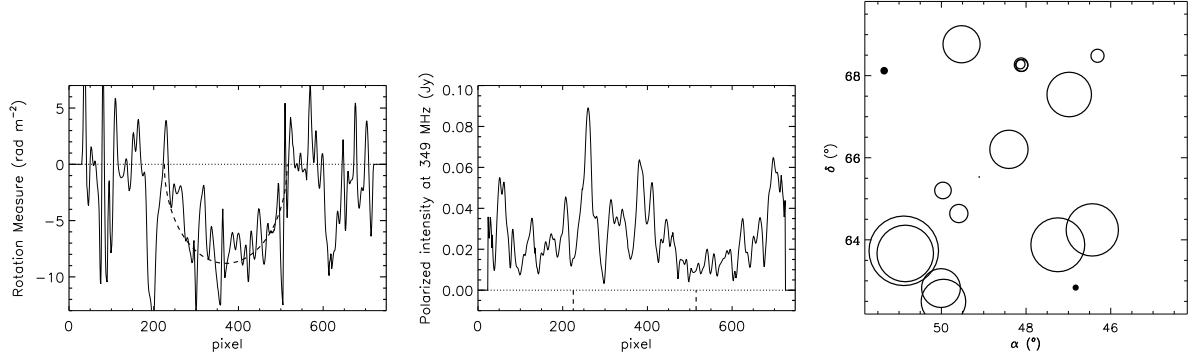


FIGURE 4. *Left and center:* horizontal cross sections through the RM map and the P map of the Horologium field in Fig. 3 (at $4'$ resolution) through the center of the RM disk. The dashed line in the RM plot is a fit to the decrease in RM, calculated for a sphere of constant thermal electron density and line-of-sight magnetic field. In the P plot, the same fit is indicated at the bottom. *Right:* RM's of observed polarized extragalactic point sources in the Horologium field. The radii of the circles are again scaled with magnitude of RM, but with radii twice as small as in Fig. 2. Maximum (minimum) RM is 7.4 (-67.9) rad m $^{-2}$.

RM's of these sources are in the range of -67.9 to 7.4 rad m $^{-2}$. These RM values are not correlated with the RM's from the diffuse radiation, similar as in the Auriga field. Extragalactic source RM's are higher than in the Auriga field, which is most likely due to the lower latitude of the Horologium field.

INTERPRETATION OF THE OBSERVATIONS

The galactic synchrotron emission is thought to originate from two separate domains centered on the galactic plane: a thin and a thick disk, with scale heights of 180 pc and 1.8 kpc respectively ([15]). The thick disk emits 90% of the synchrotron radiation, and the thin disk coincides approximately with the stellar disk and the HI disk. Pulsar RM observations have shown that the random magnetic field in the thin disk $B_{ran} \approx 5\mu\text{G}$ is of the same order or larger than

TABLE 1. Three schematic domains with different characteristics in the galactic ISM and halo.

| domain | components | scale height (pc) | relevant constituents | $B_{\text{ran}}/B_{\text{reg}}$ |
|--------|----------------|-------------------|-----------------------|------------------------------------|
| III | Reynolds layer | Thick disk | 1800 | n_{rel}, B |
| II | | | 1000 | $n_{\text{rel}}, B, n_{\text{th}}$ |
| I | Thin disk | | 180 | $n_{\text{rel}}, B, n_{\text{th}}$ |

the regular magnetic field ([16],[17]).

The thermal electrons that cause the Faraday rotation of the synchrotron background are contained in the Reynolds layer, with a scale height of about a kpc ([18]). The thermal electrons are more confined to the galaxy than the relativistic electrons, so there is a “halo” above the Reynolds layer that only contains relativistic but no thermal electrons.

These two media thus define three domains in the galactic ISM and halo with different characteristics, as sketched in Table 1. The thin synchrotron disk (domain I) extends to a few hundred parsec, and is mixed with the lower parts of the Reynolds layer and the thick disk. The Local Bubble is not taken into account. The upper part of the Reynolds layer is also mixed with the thick synchrotron disk (domain II), whereas the highest part of the thick synchrotron disk is so high above the galactic plane that it doesn’t contain a significant amount of thermal electrons anymore (domain III). Our observations, in particular the very low upper limit on small-scale structure in total intensity I , put strict constraints on the characteristics of these three domains.

The first constraint is a small scale height of the thin disk. Due to the large random magnetic field component in the thin disk, the emissivity I has a fluctuating component. If the observed integrated emissivity of this fluctuating component is only a few Kelvin, the I -structure can be averaged out if it is on small enough scales, i.e. if there are enough “turbulent cells” along the line of sight. Therefore only a thin layer is allowed where the B_{ran} component is large, with structure on small enough scales to average out the small-scale structure in I that is created in this layer. Typically, in a layer with a scale height of 200 pc, B_{ran} -structure on scales of 10 to 20 pc can smooth I down to the observed limits.

The second constraint is a constraint on the magnetic field in the layers above the thin synchrotron disk. Small-scale structure in I emitted in these layers has to be negligible. Assuming equipartition in energy between the relativistic electrons and magnetic field, the synchrotron emissivity $\epsilon \propto B^2$. As the fluctuation in I requires $\Delta\epsilon < 1\%$, this implies that $B_{\text{ran}}/B_{\text{reg}} < 0.1$. Therefore, the absence of small-scale structure in I dictates a regular magnetic field dominating over the random magnetic field component by more than a factor ten in the halo of the galaxy, i.e. above a scale height of a few hundred parsecs, at least for the component of the magnetic field perpendicular to the line of sight.

The observed structure in polarized intensity is made by depolarization on small scales in the layers containing thermal electrons, by three mechanisms. The first mechanism is beam depolarization, as discussed above. Second, linearly polarized radiation emitted at different depths is Faraday-rotated by different amounts (differential Faraday rotation [19]) and third, small-scale structure in thermal electron density and/or magnetic field causes spatial structure in Faraday rotation (internal Faraday dispersion [20]). These depolarization mechanisms define a wavelength dependent Faraday depth for the polarized radiation, which indicates that most of the observed polarized intensity comes from the nearer part of the medium. This explains the difference between RM structure from the diffuse emission and from extragalactic point sources, as the latter is built up over the whole path length through the Faraday-rotating medium (domains I and II). A more quantitative discussion can be found in Haverkorn et al. ([10]).

CONCLUSIONS

We observed two fields of over 50 square degrees, both located in the second galactic quadrant at positive latitude, in the constellations Auriga and Horologium. All four Stokes parameters were derived from observations done at five frequencies 341, 349, 355, 360, and 375 MHz simultaneously. The total intensity I emission is featureless on scales smaller than approximately a degree, while linear polarizations Q and U show abundant structure on arcminute to

degree scales. Polarized intensity has a maximum $T_{b, pol} \approx 15 - 18$ K.

The observed structure in polarized intensity P is 'cloudy' on scales from arcminutes up to a degree. Long canals of one synthesized beam wide where no polarization is detected are caused by beam depolarization in a beam which separates two regions where the polarization angle changes abruptly by 90° (or $270^\circ, 540^\circ$ etc).

Values of RM in the two fields are in general small: $|RM| < 15$ rad m $^{-2}$. RM maps show coherent structure in RM over several independent beams up to a degree, but also sudden large RM changes across one beam of more than 100%. Not only the magnitude of the RM changes but regularly also the sign, which is most easily explained by a change in direction of B_{\parallel} . In the Horologium field, a ring-like structure in polarized intensity coincides with a disk of radially increasing RM, although the RM disk is slightly larger than the ring in P .

The lack of observed small-scale structure in total intensity I puts constraints on the medium (the galactic ISM and halo). In the thin disk of synchrotron radiation, comparable to the stellar and HI disk, the random magnetic field component B_{ran} is comparable to or larger than the regular field component B_{reg} . As B_{ran} causes fluctuating I , the layer cannot be thicker than a few hundred parsecs, and the structure has to be on small enough scales to average out the created I fluctuations. Furthermore, in the thick synchrotron disk above the thin disk, the random magnetic field has to be very small: $B_{ran} \leq 0.1 B_{reg}$. Because of depolarization in the synchrotron emitting and Faraday-rotating medium most of the polarized emission we observe originates from the nearby medium. As the RM of an extragalactic point source is built up along the entire path length through the medium, the RM structure of the diffuse emission can be uncorrelated with the structure in RM values of extragalactic point sources, as is observed.

ACKNOWLEDGMENTS

The Westerbork Synthesis Radio Telescope is operated by the Netherlands Foundation for Research in Astronomy (ASTRON) with financial support from the Netherlands Organization for Scientific Research (NWO). This work is supported by NWO grant 614-21-006.

REFERENCES

1. Wieringa, M. H., de Bruyn, A. G., Jansen, D., Brouw, W. N., and Katgert, P., *Astronomy and Astrophysics*, **268**, 215 (1993).
2. Uyaniker, B., Fürst, E., Reich, W., Reich, P., and Wielebinski, R., *Astronomy and Astrophysics Supplement Series*, **138**, 31 (1999).
3. Gray, A. D., Landecker, T. L., Dewdney, P. E., Taylor, A. R., Willis, A. G., and Normandeau, M., *Astrophysical Journal*, **514**, 221 (1999).
4. Gaensler, B. M., Dickey, J. M., McClure-Griffiths, N. M., Green, A. J., Wieringa, M. H., and Haynes, R. F., *Astrophysical Journal*, **549**, 959 (2001).
5. Duncan, A. R., Haynes, R. F., Jones, K. L., and Stewart, R. T., *Monthly Notices of the Royal Astronomical Society*, **291**, 279 (1997).
6. Katgert, P., and de Bruyn, A. G., "Small-scale structure in the diffuse polarized radio background: WSRT observations at $\lambda \approx 90$ cm", in *New Perspectives on the Interstellar Medium*, edited by A. R. Taylor, T. L. Landecker, and G. Joncas, Astronomical Society of the Pacific, 1999, p. 411.
7. Haslam, C. G. T., Stoffel, H., Salter, C. J., and Wilson, W. E., *Astronomy and Astrophysics Supplement Series*, **47**, 1 (1982).
8. Roger, R. S., Costain, C. H., Landecker, T. L., and Swerdllyk, C. M., *Astronomy and Astrophysics Supplement Series*, **137**, 7 (1999).
9. Haverkorn, M., Katgert, P., and de Bruyn, A. G., *Astronomy and Astrophysics*, **4**, L245 (2000).
10. Haverkorn, M., Katgert, P., and de Bruyn, A. G., *Astronomy and Astrophysics* (2002), submitted.
11. Sokoloff, D. D., Bykov, A. A., Shukurov, A., Berkhuijsen, E. M., Beck, R., and Poezd, A. D., *Monthly Notices of the Royal Astronomical Society*, **299**, 189 (1998).
12. Leahy, J. P., *Monthly Notices of the Royal Astronomical Society*, **226**, 433 (1987).
13. Brouw, W. N., and Spoelstra, T. A. T., *Astronomy and Astrophysics Supplement Series*, **26**, 129 (1976).
14. Verschuur, G. L., *The Observatory*, **88**, 15 (1968).
15. Beuermann, K., Kanbach, G., and Berkhuijsen, E. M., *Astronomy and Astrophysics*, **153**, 17 (1985).
16. Rand, R. J., and Kulkarni, S., *Astrophysical Journal*, **343**, 760 (1989).
17. Ohno, H., and Shibata, S., *Monthly Notices of the Royal Astronomical Society*, **262**, 953 (1993).
18. Reynolds, R. J., *Astrophysical Journal*, **339**, 29 (1989).
19. Gardner, F. F., and Whiteoak, J. B., *Annual Review of Astronomy and Astrophysics*, **4**, 245 (1966).
20. Burn, B. J., *Monthly Notices of the Royal Astronomical Society*, **133**, 67 (1966).